

Investigation of the electronic structure, magnetic, and optical characteristics of Ni-doped boron nitride nanotube

Sabah S. Farhan^{1*}

¹Department of Physics, College of Science, University of Anbar, Ramadi, Iraq

ARTICLE INFO

Received: 28/01/2025
Accepted: 03/03/2025
Available online: 14/11/2025
December Issue
[10.37652/juaps.2025.157003.1352](https://doi.org/10.37652/juaps.2025.157003.1352)

 CITE @ JUAPS

Corresponding author

Sabah S. Farhan
sabah.falahi@uoanbar.edu.iq

Keywords: BNNT, DFT, Electrical characteristics, Nanocomposite

ABSTRACT

First-principles density functional calculations were implemented to study the electronic structure, optical, and magnetic properties of (10,0) Ni-combined boron nitride BN nanotubes. BNNTs were substituted with Ni to afford the formula B_{1-x}Ni_xN at (x) contents of 0.05, 0.10, 0.15, 0.20, and 0.25. The obtained calculations showed that pristine BNNTs have an extensive band gap of 4.12 eV. Incorporating Ni atoms in the BNNTs reduced the energy gap by generating additional states beyond the Fermi level in the conduction band. Additionally, nickel dopants can cause magnetism in BNNTs, leading to a split in the density of states. The polarized DOS diagram typically displays noticeably different distributions, indicating that the Ni-incorporated material exhibits magnetic properties. Optical calculations revealed that the pristine BNNT does not have an absorption edge in the visible light region. Introducing Ni can increase the absorption coefficient of B_{1-x}Ni_xN nanotubes in the visible and infrared regions of the spectrum, thereby enhancing the material's ability to conduct electrical current.

1 INTRODUCTION

Group III-V semiconductors have garnered significant attention due to their exceptional optoelectronic properties. Among these materials, the boron nitride BN has attracted notable interest due to its significant properties such as high thermal and chemical stability, high mechanical rigidity, low dielectric constant, and very low coefficient of friction [1]. There are different structural forms of boron nitride, such as bulk BN (hexagonal (h-BN) and cubic (c-BN)), boron nitride nanosheets (BNNSs), and boron nitride nanotubes (BNNTs). Boron nitride nanotubes are a type of one-dimensional nanostructured material. These materials are structurally similar to carbon nanotubes because they substitute boron and nitrogen atoms instead of carbon atoms. BNNTs have a wide energy gap of approximately 5 eV [2]. The wide band gap of BNNTs results from the partial ionic character of the (B-N) bond because of the differences in electronegativity of the two elements [3]. Since nitrogen

is more electronegative than boron, it attracts electrons closer to itself, creating a partial ionic bond [4].

This difference in electronegativity results in a bond that is not covalent but rather highly ionic. This ionic property results in a large energy separation between the valence and conduction bands [5]. In partial ionic bonds, the required energy to motivate an electron from the valence band (VB) to the conduction band (CB) is much greater than that in covalent bonds. This high energy requirement is the reason for the wide band gap in BNNTs. These wide band gaps have multiple applications, including optoelectronics, nanocomposites, thermal insulators, and optical and biomedical applications.

Reducing the energy gap of boron nitride nanotubes may have numerous benefits, including enhancing electrical conductivity and improving optoelectronic devices, as well as improving interactions with biological systems and expanding the applications of nanocomposites. Several methods have been used to reduce the energy gap of BNNTs. Among these methods, doping involves the

common technique of modifying a material's electronic properties [6,7]. Substitutional doping involves incorporating foreign atoms into the BNNT structure, altering its electronic properties and reducing the band gap. This technique can also change the optical properties of the structure [8]. The doping of BN nanotubes can modify their energy gap, resulting in a decrease in energy consumption. This makes the BN nanotubes more conductive and improves their ability to absorb light in various spectral regions [9].

Common dopants include carbon (C), oxygen (O), iron (Fe), cobalt (Co), nickel (Ni), and manganese (Mn). In recent years, experimental and theoretical investigations into the electronic structure, magnetic, and optical properties of doped BNNT systems have been conducted. da Silva et al. prepared and studied the effect of samarium-doped boron nitride nanotubes [10]. Pi et al. investigated the ability of Ni-doped BNNTs to sense decomposed SF₆ components [11]. Yuksel et al. applied DFT calculations to study the adsorption and sensing of 5-fluorouracil by Ni-doped boron nitride nanotubes [12]. Wang et al. applied DFT calculations to determine the adsorption of TCDD on Ni-doped BNNTs [13]. Habibi-Yangjeh and Basharnavaz calculated the adsorption of HCN molecules on Ni-doped BNNTs [14]. Tontapha et al. applied DFT to investigate CO adsorption on Ni-doped boron nitride nanotubes [15].

This study used first-principles calculations to investigate the electronic structure, optical, and magnetic properties of Ni-combined BN nanotubes. Doping with metal reduces the band gap of BN nanotubes, thereby increasing their conductivity. Depending on the doping of the metal, nanotubes can transform from insulating to semiconducting or metallic conductors. Naturally, BN nanotubes are nonmagnetic structures. Doping with transition metals (such as iron, cobalt, and nickel) can result in magnetic properties. The incorporation of these metal atoms can generate local magnetic moments in the BN lattice, leading to ferromagnetism or other magnetic behaviors. Metal doping can produce new energy levels within the band, improving optical properties, and might be useful for optoelectronic applications.

2 MATERIALS AND METHODS

2.1 Computational details

The electronic structure, optical, and magnetic characteristics of 10,0 BNNTs were calculated using density functional theory (DFT). The pristine structure consisted

of 20 boron atoms and 20 nitrogen atoms, as illustrated in Figure 1. For incorporation, one of the boron atoms was replaced by one of the considered nickel atoms. Boron nitride nanotubes were substitutional doped with Ni to afford B_{1-x}Ni_xN at (x) contents of 0.05, 0.10, 0.15, 0.20, and 0.25. The generalized gradient approximation (GGA) with the Perdew–Burke–Ernzerhof exchange–correlation functional was used. Our calculations were performed using "SIESTA" package [16]. The nanotube structures were completely optimized until the force on each atom was less than 0.04 eV/Å. The Brillouin zone is sampled by the Monkhorst-Pack scheme as 6 × 1 × 1 k-points along the tube axis. The calculations were performed with a vacuum width of 15 Å to avoid interactions between the surrounding structures. The energy cutoff for the charge density and the wavefunction was considered to be 200 Ry. The optical mesh size was 33 × 1 × 1 for a one-dimensional nanotube.

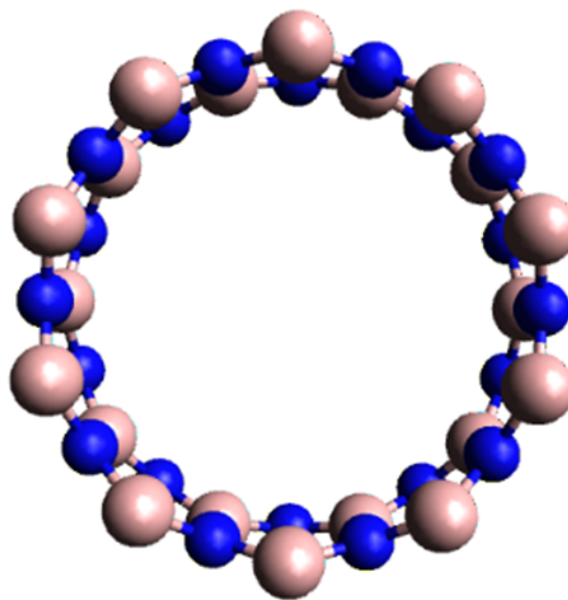


Fig. 1 The pristine structure of the BN nanotube

The dielectric function was considered to determine the optical parameters.

$$\varepsilon = \varepsilon_1 + i\varepsilon_2 \quad (1)$$

where ε_1 and ε_2 refer to the real and imaginary parts of the complex dielectric function, respectively, which can be obtained from the Kramers-Kronig transform [17]:

$$+\frac{2}{\pi} \mathbf{P} \int_0^{\infty} \frac{\omega' \varepsilon_2}{\omega'^2 - \omega^2} d\omega' \quad (2)$$

$$\varepsilon_2 = \frac{e^2 \hbar}{\pi m^2 \omega} \sum_{i,j} |\rho_{ij}|^2 \delta(E_j^k - E_i^k - \hbar\omega) d^3\omega \quad (3)$$

where P is Cauchy's principal value of the integral, ρ_{ij} is the dipole transition matrix element, E_i^k and E_j^k are the first and final energy states of an electron with wavevector k , and $\hbar\omega$ is the photon energy.

The dielectric function components play a significant role in determining various optical parameters of materials. Light and material can collaborate through a wide range of wavelengths and frequencies. These parameters were employed to calculate several optical properties such as reflectivity (R), the absorption coefficient (α), refractive index (n), power loss function (L), and optical conductivity (σ). These parameters can be considered by carrying out equations (4-8) [18]:

$$\alpha = \sqrt{2}\omega \left(\sqrt{\varepsilon_1^2 + \varepsilon_2^2} - \varepsilon_1 \right)^{1/2} \quad (4)$$

$$R = \left| \frac{\sqrt{\varepsilon} - 1}{\sqrt{\varepsilon} + 1} \right|^2 \quad (5)$$

$$n = \left(\frac{\sqrt{\varepsilon_1^2 + \varepsilon_2^2} + \varepsilon_1}{2} \right)^{1/2} \quad (6)$$

$$\sigma = \frac{-i\omega}{4\pi} |\varepsilon - 1| \quad (7)$$

$$L = \frac{\varepsilon_2}{\varepsilon_1^2 + \varepsilon_2^2} \quad (8)$$

3 RESULTS AND DISCUSSION

3.1 Electronic structure

The electronic structures of zigzag (10,0) $B_{1-x}Ni_xN$ nanotubes at various (x) rates were investigated. Before calculating the electronic structure and magnetic properties, structural optimization of $B_{1-x}Ni_xN$ was performed. The optimization of the system was achieved 1000 times to obtain the best relaxed state. The energy-K-point (E-K) diagram was used to investigate the electronic properties of the system. The (E-K) displays the permitted energy levels for electrons in many regions of the Brillouin zones. Figure 2 (a-f) illustrates the band structure and associated density of states of $B_{1-x}Ni_xN$ ($x = 0.05, 0.10, 0.15, 0.20$, and 0.25). The energy gap of the pristine BNNTs was 4.12 eV, which is in good agreement with the theoretical data obtained

by Movlareoy, and Minaie [2]. However, this is still less than the experimental results at approximately 5 eV. This is due to the use of the GGA-PBE approximation. GGA with the PBE function is known to reduce the energy gap in materials. The GGA-PBE function does not completely correct self-interaction errors when an electron incorrectly interacts with itself. This error can lead to a further reduction in the band gap. When the Ni atom in the BNNTs substitutes for the B atom, it generates additional states within the Fermi level that are located in the conduction band, thereby reducing the energy gap. Generating these new states could shift the Fermi level closer to the CB. This shift means that electrons can be thermally excited into the conduction band more easily. Table 1 displays the values of the energy gap of $B_{1-x}Ni_xN$ at various (x) rates.

Table 1 Energy gaps of the $B_{1-x}Ni_xN$ nanotubes at various (x) rates

X	E _g eV
0.00	4.12
0.05	3.92
0.10	3.67
0.15	2.62
0.20	2.43
0.25	2.28

To investigate the magnetic properties of the $B_{1-x}Ni_xN$ nanotubes, the polarized density of states (DOS) of these systems was calculated. The density of polarized states is a concept used to describe the distribution of electronic states in a spin-polarized material. This means that the electronic states differ for electrons with spins aligned in various directions. In ferromagnetic materials, the spins are spontaneously aligned in the same direction that resulting in a net magnetic moment. Magnetic materials typically exhibit an imbalance between the up- and down-spin states, indicating the material's magnetization. In antiferromagnetic materials, adjacent spin states line up in opposite directions, resulting in no net magnetic moment. The system may show similar densities for spin-up and spin-down states. The spin states are randomly oriented in paramagnetic materials but can align in an external magnetic field. The density of polarized states in paramagnetic materials does not differ significantly between spin-up and spin-down states without an external magnetic field. Figure 3 (a-f) shows

the polarized DOS of the $B_{1-x}Ni_xN$ nanotube at various (x) rates. pristine BNNTs are nonmagnetic materials since the spin-up and spin-down DOSs are usually symmetric. This result is connected with the data gained by Pantha et al. [19]. Nickel dopants can induce magnetism in BNNTs, leading to a split in the density of states for spin-up and spin-down electrons. The polarized DOS diagram typically exhibits noticeably different distributions, indicating that the material possesses magnetic properties.

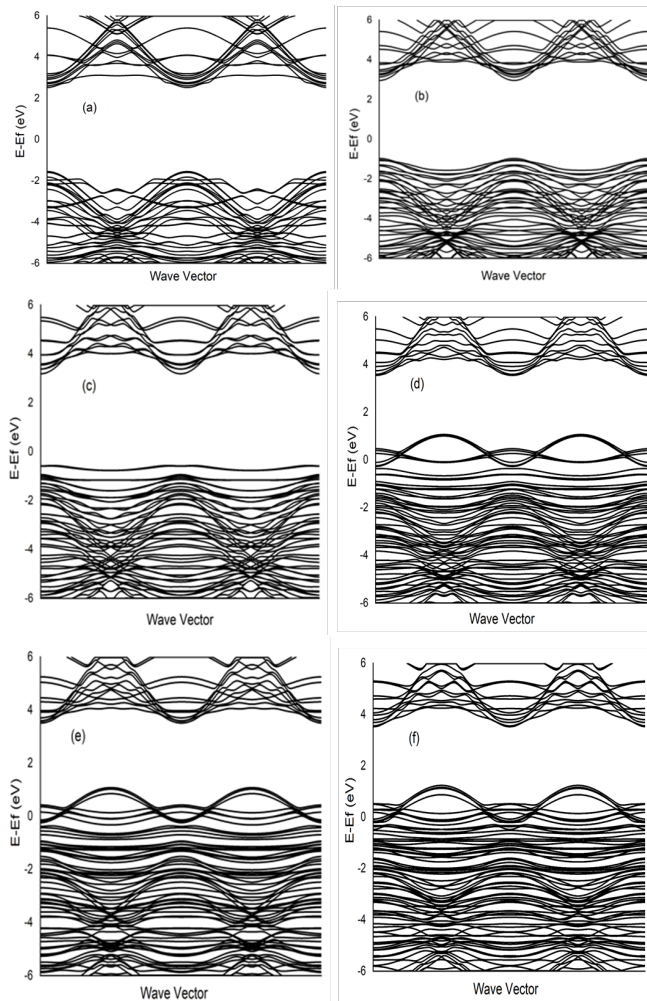


Fig. 2 Band structure and associated density of states of $B_{1-x}Ni_xN$ for various x values (a 0.00, b: 0.05, c: 0.10, d: 0.15, e: 0.20, and f: 0.25)

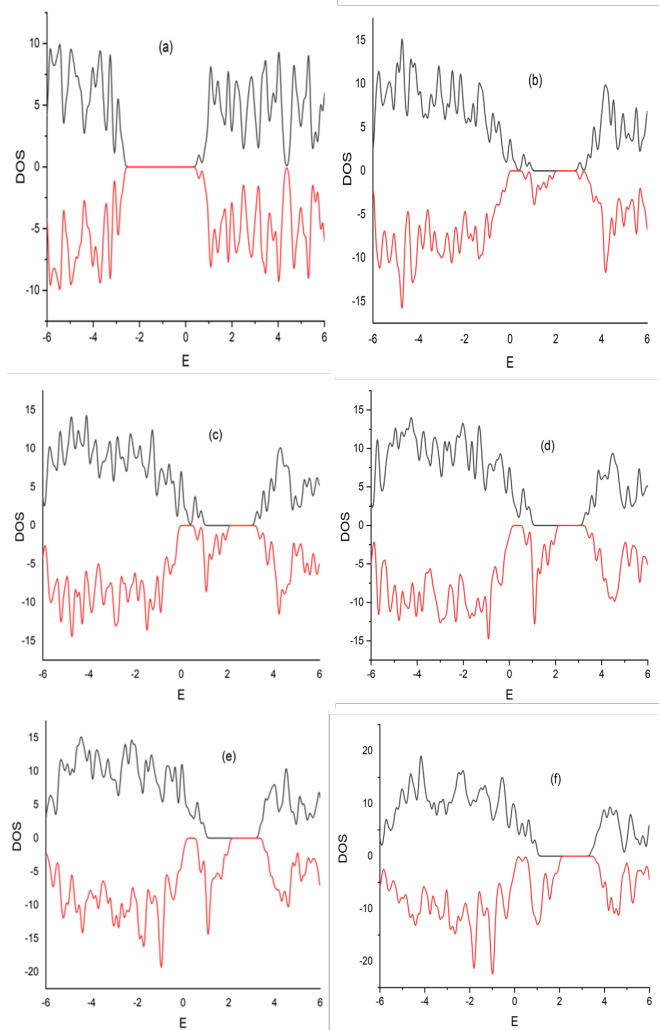


Fig. 3 (a-f) Polarized DOS of the $B_{1-x}Ni_xN$ nanotubes at various (x) rates (a: 0.00, b: 0.05, c: 0.10, d: 0.15, e: 0.20, f: 0.25)

3.2 Optical properties

In this section, the optical properties of the $B_{1-x}Ni_xN$ nanotubes from density functional theory (DFT) calculations were investigated using the complex dielectric function, which contains real and imaginary parts from the Kramers–Kronig transformation [20]. The calculated real part of the dielectric function of the $B_{1-x}Ni_xN$ nanotube is shown in Figure 4. The maximum peak in the real part of the spectrum of the pristine BNNTs occurred at a wavelength of 308 nm in the UV region. The risky UV region refers to the part of the ultraviolet spectrum that poses potential health risks to humans due to its high-energy radiation. This result is associated with the data obtained by Satawara et al. [21]. Additionally, ϵ_1

increases in the middle of the UV region. At that point, it quickly decreases in the wavelength range of 310-466 nm. ϵ_1 increases with increasing Ni content in $B_{1-x}Ni_xN$ in the wavelength range of 574-1190 nm.

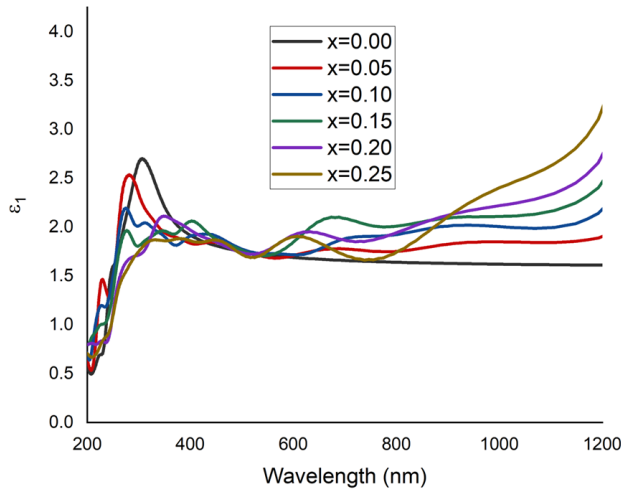


Fig. 4 Real parts of the dielectric functions of the $B_{1-x}Ni_xN$ nanotubes at various (x) rates

ϵ_2 indicates the energy loss of the electric field as it propagates through the material. Figure 5 illustrates ϵ_2 of the $B_{1-x}Ni_xN$ nanotube at various (x) rates. The highest peak occurring at ϵ_2 is consistent with the result obtained by Satawara et al. [21]. ϵ_2 increases with increasing Ni content in $B_{1-x}Ni_xN$ in the wavelength range from 333-1190 nm.

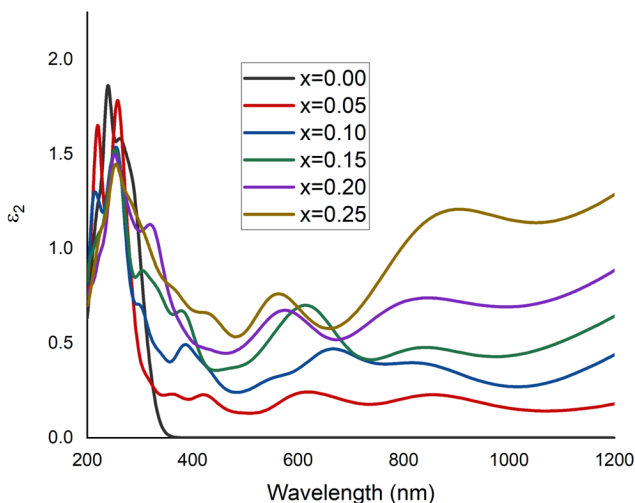


Fig. 5 ϵ_2 of the $B_{1-x}Ni_xN$ nanotube at various (x) rates

The absorption coefficient reflects the decrease in the intensity of the incident light that passes through the material. The absorption coefficient relies on the material type and the wavelength of the absorbed light [22]. Figure 6 displays the absorption of the $B_{1-x}Ni_xN$ nanotubes at various (x) rates. The absorption peak for pristine BNNTs regularly appears in the deep-UV region at approximately 200-250 nm. The pristine BNNT does not have any absorption edge in the visible light region. This result is consistent with the results of Satawara et al. [21]. This makes BNNTs valuable in applications such as UV lasers and UV light detection, as well as a protective coating against UV radiation. Increasing the Ni content in $B_{1-x}Ni_xN$ shifted the absorption coefficient peaks toward regions of low wavelength. Introducing metals such as Ni can increase the absorption coefficient of $B_{1-x}Ni_xN$ nanotubes in the deep-UV region of the spectrum.

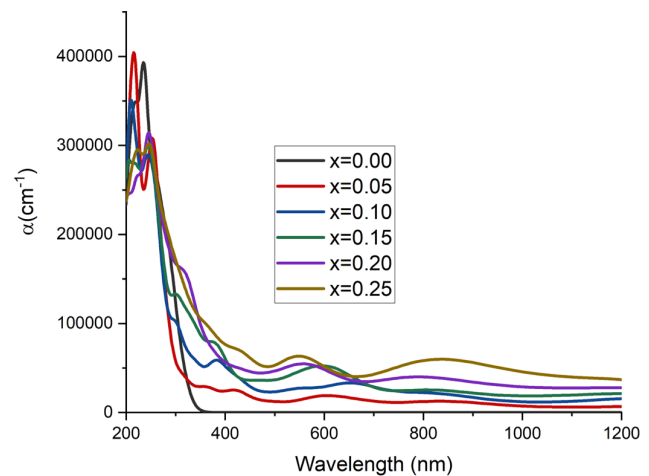


Fig. 6 The absorption of $B_{1-x}Ni_xN$ nanotubes at various (x) rates

Optical conductivity defines a material's response to an electromagnetic field. The optical conductivity of the $B_{1-x}Ni_xN$ nanotubes is shown in Figure 7. Pristine BNNT showed a prominent sharp peak at a wavelength of 239 nm. Its transparency is considered to be in the visible range, and its strong absorption occurred in the ultraviolet (UV) region. Incorporating BNNTs with Ni introduced additional electronic states within the band gap, thereby reducing the band gap and enhancing the material's ability to conduct electrical current.

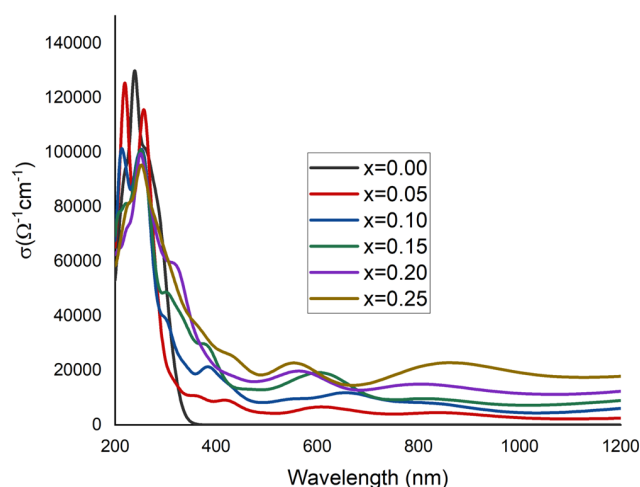


Fig. 7 Optical conductivity of $B_{1-x}Ni_xN$ nanotubes at various (x) rates

4 CONCLUSION

The electronic structure, optical, and magnetic properties of substitutional doped Ni in (10,0) BN nanotubes were studied in detail. Our calculations revealed that incorporating Ni atoms into BNNTs reduces the energy gap. Additionally, nickel dopants can split the density of states of BNNTs, indicating that the Ni-incorporated material exhibits magnetic properties. Introducing Ni can increase the absorption coefficient of $B_{1-x}Ni_xN$ nanotubes in the visible and infrared regions of the spectrum, thereby enhancing the material's ability to conduct electrical current. These improved electrical properties make Ni-doped BNNTs candidates for use in nano-electronic devices, such as transistors and sensors. The improved magnetic properties also make them suitable for spintronic devices, where the spin of electrons is utilized for information processing.

ACKNOWLEDGEMENT

We acknowledge the department of physics, College of Science, University of Anbar for their appreciated support for this research.

FUNDING SOURCE

No funds received.

DATA AVAILABILITY

N/A

DECLARATIONS

Conflict of interest

The authors declare that they have no known competing financial interests or personal relationships that could have appeared to influence the work reported in this paper.

Consent to publish

All authors consent to the publication of this work.

Ethical approval

N/A

REFERENCES

- [1] Roy S, Zhang X, Puthirath AB, Meiyazhagan A, Bhattacharyya S, Rahman MM, et al. Structure, Properties and Applications of Two-Dimensional Hexagonal Boron Nitride. *Advanced Materials*. 2021;33(44). [10.1002/adma.202101589](https://doi.org/10.1002/adma.202101589)
- [2] Movlaroooy T, Minaie B. First principles study of structural and electronic properties of BN-NTs. *Journal of Computational Electronics*. 2018;17(4):1441–1449. [10.1007/s10825-018-1247-0](https://doi.org/10.1007/s10825-018-1247-0)
- [3] Kayang KW, Nyankson E, Efavi JK, Abavare EKK, Garu G, Onwona-Agyeman B, et al. Single-Walled boron nitride nanotubes interaction with nickel, titanium, palladium, and gold metal atoms-A first-principles study. *Results in Materials*. 2019;2:100029. [10.1016/j.rinma.2019.100029](https://doi.org/10.1016/j.rinma.2019.100029)
- [4] Talapunur V. Effect of molecular adsorption on the electronic structure of single walled carbon nanotubes. BITS Pilani; 2015
- [5] Wang X, Ismael A, Ning S, Althobaiti H, Al-Jobory A, Girovsky J, et al. Electrostatic Fermi level tuning in large-scale self-assembled monolayers of oligo(phenylene-ethynylene) derivatives. *Nanoscale Horizons*. 2022;7(10):1201–1209. [10.1039/d2nh00241h](https://doi.org/10.1039/d2nh00241h)
- [6] Motlak M, Hamza A, Nawaf S. Synthesis and application of Co/TiO₂ nanoparticles incorporated carbon nanofibers for direct fuel cell. *Journal of Physics: Conference Series*. 2019;1178:012006. [10.1088/1742-6596/1178/1/012006](https://doi.org/10.1088/1742-6596/1178/1/012006)
- [7] Enad AG, Abdullah ET, Hamed MG. Study the Electrical Properties of Carbon Nanotubes/Polyaniline

- Nanocomposites. *Journal of Physics: Conference Series*. 2019;1178:012032. [10.1088/1742-6596/1178/1/012032](https://doi.org/10.1088/1742-6596/1178/1/012032)
- [8] Nawaf S, Ibrahim AK, Al-Jobory AA. Electronic structure and optical properties of Fe-doped TiO₂ by ab initio calculations. *International Journal of Modern Physics C*. 2022;34(02). [10.1142/s012918312350016x](https://doi.org/10.1142/s012918312350016x)
- [9] Ravichandran K, Suvathi S, Ravikumar P, Mohan R. In: *Wide Band Gap Semiconductors*. CRC Press; 2024. p. 40–53. [10.1201/9781003450146-4](https://doi.org/10.1201/9781003450146-4)
- [10] da Silva WM, Hilário Ferreira T, de Moraes CA, Soares Leal A, Barros Sousa EM. Samarium doped boron nitride nanotubes. *Applied Radiation and Isotopes*. 2018;131:30–35. [10.1016/j.apradiso.2017.10.045](https://doi.org/10.1016/j.apradiso.2017.10.045)
- [11] Pi S, Zhang X, Chen D, Tang J. Sensing properties of Ni-doped boron nitride nanotube to SF₆ decomposed components: A DFT study. *AIP Advances*. 2019;9(9). [10.1063/1.5119873](https://doi.org/10.1063/1.5119873)
- [12] Yuksel N, Kose A, Fellah MF. A Density Functional Theory study for adsorption and sensing of 5-Fluorouracil on Ni-doped boron nitride nanotube. *Materials Science in Semiconductor Processing*. 2022;137:106183. [10.1016/j.mssp.2021.106183](https://doi.org/10.1016/j.mssp.2021.106183)
- [13] Wang R, Zhang D, Liu C. DFT study of the adsorption of 2,3,7,8-tetrachlorodibenzo-p-dioxin on pristine and Ni-doped boron nitride nanotubes. *Chemosphere*. 2017;168:18–24. [10.1016/j.chemosphere.2016.10.050](https://doi.org/10.1016/j.chemosphere.2016.10.050)
- [14] Habibi-Yangjeh A, Basharnavaz H. Adsorption of HCN molecules on Ni, Pd and Pt-doped (7, 0) boron nitride nanotube: a DFT study. *Molecular Physics*. 2018;116(10):1320–1327. [10.1080/00268976.2018.1426129](https://doi.org/10.1080/00268976.2018.1426129)
- [15] Tontapha S, Ruangpornvisuti V, Wannoo B. Density functional investigation of CO adsorption on Ni-doped single-walled armchair (5,5) boron nitride nanotubes. *Journal of Molecular Modeling*. 2012;19(1):239–245. [10.1007/s00894-012-1537-6](https://doi.org/10.1007/s00894-012-1537-6)
- [16] Soler JM, Artacho E, Gale JD, García A, Junquera J, Ordejón P, et al. The SIESTA method for ab initio order-N materials simulation. *Journal of Physics: Condensed Matter*. 2002;14(11):2745–2779. [10.1088/0953-8984/14/11/302](https://doi.org/10.1088/0953-8984/14/11/302)
- [17] Nawaf S, Rzaiz JM, Al-Jobory AA, Motlak M. Investigating the optical properties and electronic structure of gallium phosphide nanotubes doped with arsenic via implementing first-principles calculations. *Journal of Molecular Modeling*. 2024;30(8). [10.1007/s00894-024-06047-3](https://doi.org/10.1007/s00894-024-06047-3)
- [18] Nawaf S, Al-Jobory AA, Rzaiz JM, Ibrahim AK. First Principal Calculations on the Electronic Structure and the Optical Properties of Al-doped Zigzag GaN Nanotube. *Plasmonics*. 2024;19(6):3035–3042. [10.1007/s11468-024-02211-w](https://doi.org/10.1007/s11468-024-02211-w)
- [19] Pantha N, Bissokarma P, Adhikari NP. First-principles study of electronic and magnetic properties of nickel doped hexagonal boron nitride (h-BN). *The European Physical Journal B*. 2020;93(9). [10.1140/epjb/e2020-10186-2](https://doi.org/10.1140/epjb/e2020-10186-2)
- [20] Rzaiz JM, Nawaf SO, Khalaf ASM. A Study on the Scattering and Absorption Efficiencies of Si-Ag Coaxial Nanowire. *Iraqi Journal of Science*. 2019;2003–2008. [10.24996/ijs.2019.60.9.13](https://doi.org/10.24996/ijs.2019.60.9.13)
- [21] Satawara AM, Shaikh GA, Gupta SK, Gajjar PN. Structural, electronic and optical properties of hexagonal boron-nitride (h-BN) monolayer: An Ab-initio study. *Materials Today: Proceedings*. 2021;47:529–532. [10.1016/j.matpr.2020.10.589](https://doi.org/10.1016/j.matpr.2020.10.589)
- [22] Mahmood KD, Aadim KA, Hammed MG. Effect of the Pulsed Laser Energy on the Properties of CdO: NiO Composite Thin Films for Solar Cell Applications. *Iraqi Journal of Science*. 2022;1004–1017. [10.24996/ijs.2022.63.3.10](https://doi.org/10.24996/ijs.2022.63.3.10)

How to cite this article

Farhan SS. Investigation of the electronic structure, magnetic, and optical characteristics of Ni-doped boron nitride nanotube. *Journal of University of Anbar for Pure Science*. 2025; 19(2):109-115. doi:[10.37652/juaps.2025.157003.1352](https://doi.org/10.37652/juaps.2025.157003.1352)